European Journal of Chemistry

Journal webpage: www.eurjchem.com

Screening the fluid bed granulation process variables and moisture content determination of pharmaceutical granules by NIR Spectroscopy

Ahmed Shawky Abouzaid [1,2,*], Maissa Yacoub Salem [3], Eman Saad Elzanfaly [3], Ahmed Emad El Gindy [1], Stephen Hoag [2] and Ahmed Ibrahim [2]

[1] *Analytical Chemistry Department, Faculty of Pharmacy, Misr International University, Cairo, 11562, Egypt*
[2] *School of Pharmacy, University of Maryland, Baltimore, Maryland, 21201, USA*
[3] *Analytical Chemistry Department, Faculty of Pharmacy, Cairo University, Cairo, 11562, Egypt*

** Corresponding author at: Analytical Chemistry Department, Faculty of Pharmacy, Misr International University, Cairo, 11562, Egypt. Tel.: +2.02.2376023. Fax: +2.02.24772038. E-mail address: shawky0225@gmail.com (A.S. Abouzaid).*

ARTICLE INFORMATION

DOI: 10.5155/eurjchem.8.3.265-272.1608

Received: 03 July 2017
Received in revised form: 31 July 2017
Accepted: 05 August 2017
Published online: 30 September 2017
Printed: 30 September 2017

KEYWORDS

Moisture content
NIR spectroscopy
Fluid bed granulation
PLS regression model
Plackett-Burman design
Granulation process variables

ABSTRACT

The fluid bed granulation (FBG) is a wet granulation technique for producing granules. It is a complex process because many process variables can influence the granule properties. Therefore, an understanding of the influence of the granulation process variables is necessary for controlling the process. The moisture content of granule also plays a critical role in determining the outcome of the batch. The purpose of this work was to apply Plackett-Burman design for screening of process variables in FBG, study the influence of the process variables on granules properties and the use of NIR spectroscopy and partial least squares (PLS) regression to predict the moisture content of the granules. In order to study the influence of the process variables on the granules properties, Plackett-Burman design with six factors, two levels and three replicates at the center point (15 runs) was used. The results revealed that the atomizing pressure and the airflow rate are the process variables that have strong influence on the granules properties. The NIR spectroscopy in conjunction with PLS was used to determine the moisture content of granule in the FBG. The proposed PLS model was fitted and its predictive performance was evaluated by traditional chemometric criteria. The root mean square error of prediction (RMSEP) was 4.15% with 2 latent variables (LVs). The proposed NIR method was validated and the results obtained were compared with those of the reference LOD method using a paired t-test.

Cite this: *Eur. J. Chem.* **2017**, *8(3)*, 265-272

1. Introduction

Fluid bed granulation is a wet granulation technique for producing granules by spraying solution (binder solution) on to a fluidized powder. The particles in the path of the spray get wetted and collide with each other to adhere and form granules. Similar to all other wet granulation techniques, the main objectives of the FBG are to improve the flow characteristics, compression properties, increase the density, uniform blends, minimize segregation, and reduce the dust [1]. FBG is a widely applied wet granulation technique in the pharmaceutical industry, exhibiting some significant advantages compared to the multistage wet granulation methods. The mixing, spraying and drying are all carried out in single equipment, which simplifies the process [2]. Besides, it saves on labor costs, transfer losses, and time [3]. Furthermore, the granules produced by FBG were finer, more flowing and more homogenous. FBG is a complex process because there are many process variables that can influence the granule properties. Therefore, an understanding of the influence of the granulation process variables is necessary for controlling the process [4-6]. Plackett-Burman (PB) design is a widely used screening design for the identification of "main factors" that cause variability in product quality [7]. The advantage of the PB design is that many factors can be screened with a relatively few number of trials [8].

In FBG, the end-point is reached when the target granule size is reached. The granule growth is a complex process where the moisture content of granule is a critical attribute that determines granule density and granule size. The moisture content of granules also play a critical role in determining the outcome of the batch, and when moisture levels are not monitored or controlled, this could lead to over or under wetting of the powder bed resulting in batch failures. Therefore, it is critical to predict the moisture levels in the granules through the granulation process in FBG.

Near Infrared Spectroscopy (NIRS) is a rapid, nondestructive technique that requires minimal sample preparation, and can be used in-line, at-line, on-line and off-line for moisture content determination. In NIR spectroscopy [9-11], the samples are irradiated with NIR radiation. Some of this radiation is absorbed by the molecules bringing them to a higher vibrational state. Only vibrations resulting in changes in dipole moment of a molecule can absorb NIR radiation.

ISSN 2153-2249 (Print) / ISSN 2153-2257 (Online)
http://dx.doi.org/10.5155/eurjchem.8.3.265-272.1608

Table 1. The matrix of Plackett-Burman design for screening the process variables in fluid bed granulation.

Batch no	Pattern	Spraying phase			Drying phase		
		Atomization pressure (PSI)	Inlet temp. (°C)	Air flow rate (SCFM)	Inlet temp. (°C)	Air flow rate (SCFM)	Drying time (min)
1	+−+++−	9	50	12	70	12	15
2	−−+−++	5	50	12	50	12	25
3	+−−−+−	9	50	8	50	12	15
4	−−−+−−	5	50	8	70	8	15
5	000000	7	60	10	60	10	20
6	++−−−+	9	70	8	50	8	25
7	−+++−−	5	70	12	70	8	15
8	−+−−+−	5	70	8	50	12	15
9	−−+−−+	5	50	12	50	8	25
10	+−−+−+	9	50	8	70	8	25
11	000000	7	60	10	60	10	20
12	++++++	9	70	12	70	12	25
13	000000	7	60	10	60	10	20
14	−+−+++	5	70	8	70	12	25
15	+++−−−	9	70	12	50	8	15

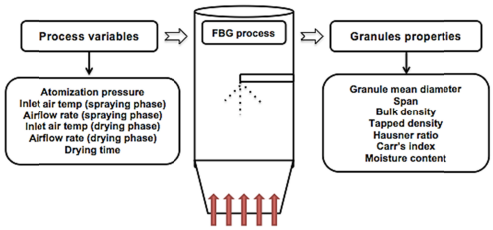

Figure 1. Fluid bed granulation; the influence of the process variable on the granule properties.

NIRS can be used for the determination of chemical properties (e.g. moisture content). It is well known that water affects the absorption intensity near 1935 nm, the well-known OH stretch region for water [12]. Several authors have reported on monitoring the moisture content of granules using NIRS in a FBG. Rantanen *et al.* [13] used three to four different wave-lengths to determine the moisture content of powder blend in the instrumented fluid bed granulator using multi-channel NIR moisture sensor. Findlay *et al.* [14] used NIR spectroscopy to simultaneously monitor moisture content and particle size in a fluid bed granulator and determine its endpoint. Hartung *et al.* [15] monitored the fluid bed granulation of an Enalapril formulation by means of in-line NIR spectroscopy with the NIR probe installed in the product container. Obregon *et al.* [16] developed a model predictive control of a fluidized bed dryer with an inline NIR as moisture sensor. The aim of this study was to screen the process variables in FBG using Plackett-Burman design and study their influence on the pharma-ceutical properties of the produced granules (Figure 1). Besides, to develop a NIR method to determine the moisture content of granule in the FBG and validate the developed method in accordance with ICH guidelines.

2. Experimental

2.1. Materials and reagents

Acetaminophen (Lot # MKBQ8028V), active ingredient was obtained from Sigma Aldrich Company, Missouri, USA. Its assay range was 99.5%. Lactose monohydrate (Lot # 1021 5919), Pharmatose® 200M was obtained from DFE Pharma, New Jersey, USA. Microcrystalline cellulose (Lot # P21382 6387), Avicel®102 and croscarmellose sodium (Lot # TN08819980) were gifted by FMC Biopolymer, Pennsylvania, USA. Magnesium stearate (Lot # L06615), Hyqual® vegetable source was obtained from MACRON Chemicals Pennsylvania, USA. Polyvinylpyrrolidone, Kollidone® K30 (Lot # G1097 6PT0) was obtained from BASF, New York, USA.

2.2. Experimental design

Construction of the experimental design, computation of coefficients and statistical parameters have been performed using JMP® software from SAS. Plackett-Burman design was applied for screening the process variables in FBG and to study the influence of the process variables on the pharmaceutical granules. Plackett-Burman design with six factors, two levels and three replicates at the center point (15 runs) was used. The granulation process variables investigated were: atomization pressure, inlet air temperature, airflow rate during the spraying phase and the inlet air temperature, airflow rate and drying time during the drying phase. The Process variables are changed according to Plackett-Burman design, as shown in Table 1.

2.3. Granulation set-up

The granulation formulation studied consisted of acetaminophen (32%, *w*:*w*) as active ingredient, lactose monohydrate (43.5%, *w*:*w*), microcrystalline cellulose (22%, *w*:*w*), croscarmellose sodium (2%, *w*:*w*), magnesium stearate (0.5%, *w*:*w*) and PVP (Kollidone® K30) in water as binder solution (15%, *w*:*v*). Appropriate quantities of active ingredient-excipients were weighted and sieved through #18 mesh before mixing in 8 qt V-blender (Patterson Kelly Company, Pennsylvania, USA) at 30 rpm for 5 min. The granulation process was performed using a Magnaflow® fluid bed processor, Model 002 (Fluid Air® Inc., Illinois, USA). The batch size was 500g. The required amount of granulation liquid consisting of 15% (*w*:*v*) solution of PVP (Kollidone® K30) in water was added during granulation at a constant spray rate of 10 mL/min. After ending the spraying of the binder solution, the granules were dried for variable time periods at different temperature (according to the PB design matrix) in the same apparatus.

2.4. Granules characterization

The properties evaluated for the granules produced during an experiment were; granule mean diameter, particle size distribution, bulk density (untapped density), tapped density, Hausner ratio, Carr's index (compressibility index), and moisture content of the granules [6]. The samples powders were manually collected from the sampling port of fluid bed granulator at regular intervals (2 min) during the granulation process. The sample size was 5 g divided into two portions; the first portion for moisture content determination and the second for particle size measurements.

2.4.1. Granule mean diameter and particle size distribution

The granule mean diameter and particle size distribution were measured by laser diffraction using the Malvern Mastersizer X/S (Malvern Inc., Worcestershire, UK) and Fraunhofer model analysis routine. The dry powder feeder was operated at an air pressure of 20 psi and a sample size of 3 g. The granule mean diameter was determined by measuring the D[4,3] which are the particle sizes at the 40th and 30th of the cumulative undersize distribution [17]. The particle size distribution is performed by determination the span according to the following equation:

$$Span = \frac{D(90)-D(10)}{D(50)} \quad (1)$$

Here, D (10), D (50) and D (90) are the particle sizes at the 10th, 50th and 90th percentiles of the cumulative undersize distribution, respectively.

2.4.2. Bulk density, tapped density, Hausner ratio and Compressibility index (Carr's index)

Granules were analyzed for bulk density, tapped density, Hausner ratio and Compressibility index, all these determinations were performed according to the USP method <616> [18] for bulk density, tapped density and USP method <1174> [18] for Hausner ratio and Compressibility index.

Bulk density and tapped density were determined using JEL Stampf®Volumeter Model STAV 2003 (Ludwigshafen, Germany). Hausner ratio (HR) is the ratio of the tapped density to its initial bulk density

$$Hausner\ ratio = \frac{\rho tapped}{\rho bulk} \quad (2)$$

A lower HR value (< 1.25) is generally an indication of good flow in accordance with USP method <1174> [18].

The compressibility Index (CI) was calculated using the values of bulk and tapped density according to the following equation:

$$Compressibility\ Index = 100 \times \frac{\rho tapped-\rho bulk}{\rho tapped} \quad (3)$$

A lower CI % value (< 20) is generally an indication of good flow in accordance with USP method <1174> [18].

2.4.3. Moisture content of the granules

The moisture content of samples was determined by loss on drying (LOD). To measure LOD, about 2 g of sample was evenly spread on the pan of the moisture analyzer (Mettler Toledo, Model HB43) and the sample weight loss was determined at 105 °C.

2.5. NIR equipment

The Metrohm NIRS XDS Rapid Content Analyzer (RCA) was used for offline NIR reflectance measurements. Samples were placed in sealed glass vials and scanned in reflectance mode over a wavelength range of 400 to 2500 nm with data collected every 0.5 nm.

2.6. Software and data analysis

Data handling, Principal component analysis (PCA) and Partial least squares (PLS) routine work were done using SOLO®8.0 (Eigenvector Research Inc., Washington, USA). PLS model was applied to the NIR spectra. In order to build PLS model, the raw data was preprocessed using one or a combination of two preprocessing methods [19]. Two types of data preprocessing, namely mean centering (MC) and auto-scaling (AS) were used in this study. The root mean square error of prediction (RMSEP) and number of latent variables (LVs) were used to evaluate the performance PLS models [20,21].

2.7. Method validation

The proposed PLS model for the NIR spectroscopy for determination the moisture content of granules was validated in accordance with ICH guidelines [22]. The method linearity, specificity, accuracy and precision (repeatability) are measured for the proposed method [23]. In addition to, the traditional chemometric criteria are calculated to evaluate the predictive ability of the developed PLS models to predict the moisture content of granules [24]. These criteria are regression coefficient (r^2), the root mean squared error of cross-validation (RMSECV) and of prediction (RMSEP) for external validation set, not involved in the calibration set.

3. Results and discussions

3.1. Analysis of the influence of the process variables on the granules properties

The Plackett-Burman design was applied for screening the process variables in fluid bed granulation and to study the influence of process variables on granules physical properties (granule mean diameter and span), granules flow properties (Hausner ratio and Carr's index) and the moisture content of the granules. The most important six process variables were investigated by Plackett-Burman design; three variables in the spraying phase (atomization pressure, airflow rate and inlet temperature) and three variables in the drying phase (airflow rate, inlet temp and drying time). Results obtained are represented in Table 2.

The regression analysis table (Table 3 and 4) was used to show the effect of the process variables on the properties of granules, it shows the contrasts (regression coefficients) of each variable, t-Ratio values and p-values to assess the significant of each variable. The t-Ratio values are calculated as Contrast/ PSE, where PSE is Pseudo Standard Error. p-Values are obtained by the *t*-test to assess the significant of each variable. *p*-Values more than 0.1 indicate that the variables are not significant. *P*-values from 0.05 to 0.10 indicate that the variables are weakly significant. While *p*-values less than 0.05 indicate that the variables are strongly significant.

3.1.1. Analysis of the influence of the process variables on the granule mean diameter and span

The airflow rate in the drying phase (*p*-value = 0.074) has a weak significant influence on granule mean diameter, as shown in Table 3a. The airflow rate in the drying phase (*p*-value = 0.099), and the interaction between the airflow rate in the spraying phase and inlet temperature in the drying phase (*p*-value = 0.085) have a weak significant influence on span, as shown in Table 3b.

Table 2. Matrix of the results after screening by Plackett-Burman design.

Batch no	Granule mean diameter (µm)	Span (µm/µm)	Moisture content (%)	Bulk density (g/mL)	Tapped density (g/mL)	Hausner ratio	Carr's index (%)
1	159.129	1.405	1.59	0.46	0.57	1.24	19
2	207.922	1.263	2.81	0.47	0.67	1.43	30
3	346.023	1.533	2.74	0.43	0.61	1.42	42
4	157.786	1.738	1.60	0.45	0.60	1.33	25
5	148.236	1.427	2.60	0.46	0.58	1.35	26
6	89.700	1.780	1.98	0.47	0.56	1.19	16
7	168.800	1.812	2.27	0.49	0.56	1.33	25
8	214.690	1.316	3.00	0.45	0.63	1.40	29
9	141.281	1.935	2.53	0.50	0.63	1.26	21
10	158.714	1.446	2.46	0.43	0.53	1.23	19
11	143.521	1.701	2.27	0.46	0.61	1.33	25
12	399.215	2.169	1.18	0.53	0.71	1.34	25
13	158.841	1.688	1.50	0.48	0.60	1.25	20
14	235.093	1.212	2.53	0.44	0.65	1.47	32
15	237.844	1.430	1.94	0.84	0.68	1.42	29

Table 3. The influence of process variables on granule mean diameter (a), span (b), bulk density (c), and tapped density (d).

Term [a]	Contrast	t-Ratio	Individual *p*-Value
Screening for granule mean diameter (a)			
X1	19.7559	0.83	0.3731
X2	13.0055	0.55	0.6169
X3	8.3618	0.35	0.7454
X4	3.0766	0.13	0.8981
X5	45.3137	1.91	0.0735 [b]
X6	-3.9017	-0.16	0.8705
X5*X5	23.7935	1.00	0.2934
X5*X1	21.7830	0.92	0.3310
X5*X2	18.7009	0.79	0.4011
X1*X2	7.6242	0.32	0.7667
X5*X3	-26.0708	-1.10	0.2550
X1*X3	-36.9951	-1.56	0.1269
Null 14	2.1077	0.09	0.9303
Null 15	1.9408	0.08	0.9343
Screening span (b)			
X1	0.036299	0.67	0.5081
X2	0.029740	0.55	0.6139
X3	0.073716	1.35	0.1687
X4	0.039131	0.72	0.4498
X5	-0.092648	-1.70	0.0989 [b]
X6	0.042560	0.78	0.4060
X5*X5	-0.007500	-0.14	0.9002
X5*X3	0.016833	0.31	0.7759
X5*X6	-0.030619	-0.56	0.6045
X3*X6	0.183212	3.36	0.0135 [c]
X5*X4	0.025538	0.47	0.6659
X3*X4	0.098347	1.81	0.0852 [b]
Null 14	-0.056079	-1.03	0.2781
Null 15	-0.006406	-0.12	0.9138
Screening for bulk density (c)			
X1	0.026833	0.92	0.3323
X2	0.035777	1.23	0.2157
X3	0.046212	1.59	0.1239
X4	-0.026833	-0.92	0.3323
X5	-0.029814	-1.03	0.2865
X6	-0.020870	-0.72	0.4588
X3*X3	0.012000	0.41	0.7039
X3*X2	0.015333	0.53	0.6296
X3*X5	-0.005715	-0.20	0.8537
X2*X5	0.014491	0.50	0.6475
X3*X1	0.047329	1.63	0.1168
X2*X1	-0.017889	-0.62	0.5710
Null 14	-0.004201	-0.14	0.8945
Null 15	0.000354	0.01	0.9924
Screening for tapped density (d)			
X1	-0.005963	-0.36	0.7404
X2	0.013416	0.80	0.3974
X3	0.017889	1.07	0.2687
X4	-0.011926	-0.71	0.4583
X5	0.020870	1.24	0.2029
X6	0.007454	0.44	0.6835
X5*X5	0.008000	0.48	0.6609
X5*X3	-0.001333	-0.08	0.9402
X5*X2	0.017419	1.04	0.2815
X3*X2	0.016102	0.96	0.3154
X5*X4	0.019720	1.18	0.2254
X3*X4	-0.010435	-0.62	0.5587
Null 14	-0.003181	-0.19	0.8568
Null 15	0.004582	0.27	0.7971

[a] X1, atomizing pressure; X2, inlet air temperature (spraying); X3, air flow rate (spraying); X4, inlet air temperature (drying); X5, air flow rate (drying); X6, drying time.
[b] Weak significant variable.
[c] Strong significant variable.

Table 4. The influence of process variables on Hausner ratio (a), Carr's index (b) and moisture content of granule (c).

Term [a]	Contrast	t-Ratio	Individual *p*-Value
Screening for Hausner ratio (a)			
X1	-0.028324	-1.34	0.1660
X2	0.017889	0.85	0.3561
X3	-0.001491	-0.07	0.9471
X4	-0.013416	-0.64	0.5446
X5	0.040249	1.91	0.0683 [b]
X6	-0.016398	-0.78	0.3982
X5*X5	0.011333	0.54	0.6202
X5*X1	-0.014667	-0.70	0.4645
X5*X2	0.002994	0.14	0.8948
X1*X2	0.010811	0.51	0.6361
X5*X6	0.050428	2.39	0.0336 [c]
X1*X6	-0.009690	-0.46	0.6735
Null 14	-0.011517	-0.55	0.6139
Null 15	-0.015514	-0.74	0.4305
Screening for Carr's index (b)			
X1	-0.89443	-0.55	0.6168
X2	0	0	1.0000
X3	-1.04350	-0.64	0.5490
X4	-1.63978	-1.00	0.2888
X5	3.13050	1.91	0.0717 [b]
X6	-1.93793	-1.18	0.2197
X5*X5	0.93333	0.57	0.6007
X5*X6	2.80000	1.71	0.0986 [b]
X5*X4	-0.51711	-0.32	0.7735
X6*X4	1.95519	1.19	0.2159
X5*X3	-2.50729	-1.53	0.1278
X6*X3	0.67082	0.41	0.7100
Null 14	0.26950	0.16	0.8791
Null 15	1.14243	0.70	0.4729
Screening for moisture content (c)			
X1	-0.212426	-2.29	0.0430 [c]
X2	-0.061865	-0.67	0.5120
X3	-0.148326	-1.60	0.1192
X4	-0.251185	-2.71	0.0280 [c]
X5	0.079753	0.86	0.3701
X6	0.026087	0.28	0.7956
X4*X4	0.038333	0.41	0.7056
X4*X1	0.042333	0.46	0.6789
X4*X3	-0.021229	-0.23	0.8318
X1*X3	-0.275687	-2.97	0.0226 [c]
X4*X5	0.111734	1.20	0.2197
X1*X5	0.007379	0.08	0.9392
Null 14	0.171531	2.22	0.0468 [c]
Null 15	-0.114287	0.12	0.9112

[a] X1, atomizing pressure; X2, inlet air temperature (spraying); X3, air flow rate (spraying); X4, inlet air temperature (drying); X5, air flow rate (drying); X6, drying time.
[b] Weak significant variable.
[c] Strong significant variable.

The interaction between airflow rate in the spraying phase with the drying time (*p*-value = 0.014) has a strong significant influence on span. The increase of airflow rate in the spraying phase with atomizing pressure allows us to obtain fine granules (small granule mean diameter) with more broadly granules dispersed (large span). This could be explained by increasing the atomization pressure decreases the moisture content of granules, which leads to a decrease in the granule size, thus obtaining granules with small mean diameter and more broadly dispersed granules (large span) [25].

3.1.2. Analysis of the influence of the process variables on the bulk and tapped density

The process variables were found to have a little influence on the bulk and tapped density which is not significant, as shown in Tables 3c and 3d. The increase of the airflow rate in the spraying phase leads to an increase in density (both bulk and tapped). This could be due to that increasing the airflow rate in the spraying phase leads to denser granules by the spatial configuration of the obtained granules.

3.1.3. Analysis of the influence of the process variables on the granule flow properties; Hausner ratio and Carr's index

To characterize granules flow properties, the Hausner ratio and compressibility index (Carr's index) were determined. The airflow rate in drying phase (*p*-value = 0.07) has a weak significant influence and the interaction between airflow rate in drying phase and drying time has a strong significant influence (*p*-value = 0.03) on the Hausner ratio, as shown in Table 4a.

The airflow rate in drying phase (*p*-value = 0.07) and the interaction between airflow rate in drying phase and drying time (*p*-value = 0.1) have a weak significant influence on the compressibility index, as shown in Table 4b.

The increase of airflow rate (drying phase) in the same time with increasing drying time leads to an increase of both Hausner ratio and Carr's index, resulting in poorer compressibility and flowability of the granules. Controversy, The increase of atomization pressure leads to granules with better compressibility and flowability properties.

Generally, the adhesion force and gravity force are significant forces that act directly on the granules during packing [26]. Therefore, the increase of airflow rate in the drying phase with the drying time leads to increase the granule attrition, resulting in a decrease the granule size and consequently, the flowability decreases. As the granule size decreases, the influence of the gravity force becomes smaller than the adhesion force, and consequently the flowability decreases [26].

3.1.4. Analysis of the influence of the process variables on the moisture content of the granules

As can be seen in Table 4c, the atomization pressure (*p*-value = 0.04), inlet air temperature in drying phase (*p*-value = 0.03) and the interaction between airflow rate in spraying phase with atomization pressure (*p*-value = 0.02) have significant influence on the moisture content of granules. As the moisture content of the granules is negatively affected by the atomization pressure, airflow rate in spraying phase and inlet air temperature in the drying phase. This could be explained by increasing the atomization pressure leads to decrease the droplet size, resulting in a decrease in the moisture content of granules. Besides, increasing the inlet air temperature (drying phase) leads to increase in the evaporation rate, resulting in a decrease in the moisture content of granules. Null 14 (uncontrolled factor) was added after all factors (process variables) were exhausted. Null 14 (*p*-value = 0.05) has a significant influence on the moisture content. As the Null 14 positively affects the moisture content of granules. This may be due to the relative humidity of the uncontrolled inlet air.

3.2. Moisture content determination by NIR Spectroscopy

3.2.1. NIR spectra

The raw NIR spectra obtained during the granulation process (spraying and drying phase) were analyzed to identify spectral features corresponding to the moisture content, as shown in Figure 2a. Peaks corresponding to the wavelength region around 1450 nm relates to the first overtone of the -OH group. Spectra regions from 1600-1800 nm corresponds to the first overtone from -CH, -CH_2, and -CH_3 and in the region 1870-1970 nm, the peak corresponds to combination band of water; increases during the spraying phase and decreases during the drying phase, as shown in Figure 2b.

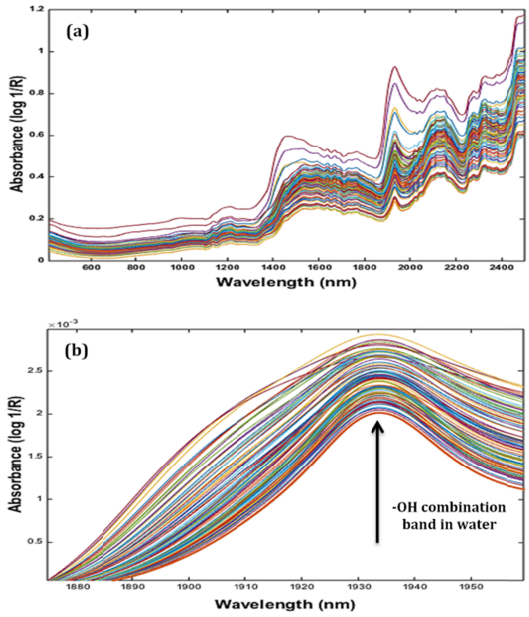

Figure 2. (a) Raw NIR spectra of the calibration samples. (b) The spectral wavelength range (1870-1970 nm) was selected, corresponding to OH combination band in water.

3.2.2. Model calibration

Spectra regions from 1870-1970 nm of the calibration and validation samples were analyzed using PCA where 2 PC's explained 100% variability in the data with PC1 and PC2 capturing 99.90%, and 0.10% variability, respectively as shown in Figure 3a. PC 1 loading plot shows maxima at 1935 nm which resembles the water peak, as shown in Figure 3b. Therefore, the spectral range was selected between 1870-1970 nm to build the PLS model. PLS models were developed using NIR spectra acquired from 100 calibration samples obtained from fifteen granulation batches with corresponding primary laboratory values (the moisture content (%) from LOD). The samples were inspected for outliers before calibration model development. In order to build PLS model, the raw data was preprocessed using different spectral preprocessing methods to remove the irrelevant spectral part in experimental data. The selected PLS model was the one obtained by applying the mean centering (MC) as it decreased the number of latent variables used by 60% (from 5 LVs to 2 LVs), as shown in Table 5.

Table 5. The performance of different tested PLS models for NIR moisture model.

PLS models *	LV	RMSEC (%)	RMSECV (%)	RMSEP (%)
Raw data	5	3.55	3.93	2.50
AS	3	3.97	4.19	3.17
MC **	2	4.30	4.46	4.15

* Selected wavelength (1870-1970 nm).
** Selected pre-processing method.

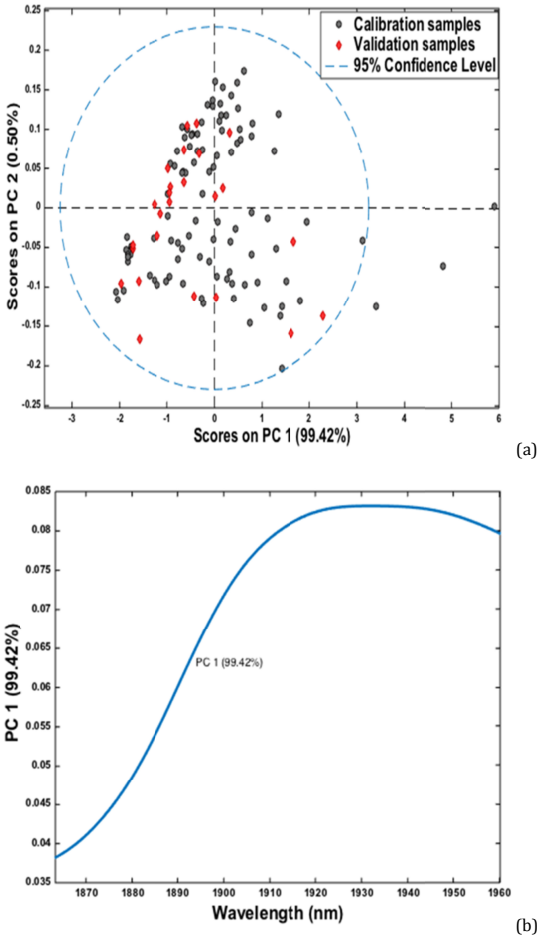

Figure 3. (a) PC1 versus PC2 score plot for the NIR spectra of the calibration and validation samples. (b) Loadings plot of PC1 showing the maxima at 1935 nm and demonstrating the specificity of PC1 to water peak.

The selected PLS model was constructed to predict the moisture levels in the fluid bed granulator.

Figure 4 is the relationship between NIR predicted and LOD% values and the calibration model resulting in R^2, RMSEC, and RMSECV values of 0.958, 4.30%, and 4.46%, respectively.

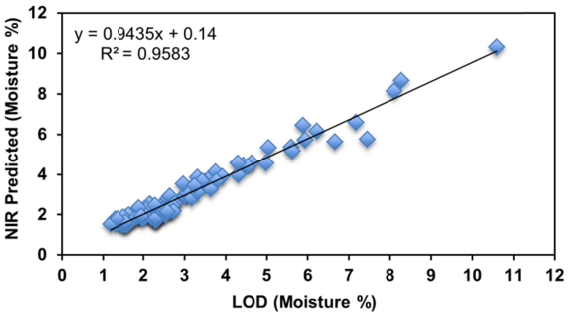

Figure 4. Regression plot between the moisture (%) predicted by NIR and the measured by LOD in the calibration set using PLS model.

3.2.3. Model validation

To validate the model, the moisture content of an external data set (25 samples) not used in the calibration model was predicted which resulted in RMSEP value of 4.15% and the regression coefficient (r^2) was 0.988.

The linearity of the proposed method was demonstrated by establishing the prediction plot between the moisture content (%) predicted by the model and those determined by the reference LOD method for the twenty five validation samples, as shown in Figure 5. The intercept, the slope and R^2 values are represented in Figure 5. The range of the proposed method was determined by the LOD method (%) values of the extreme samples (lower and upper) in the calibration set, which was 1.18 (%) and 10.59 (%), respectively. The proposed NIR method is only valid within this range.

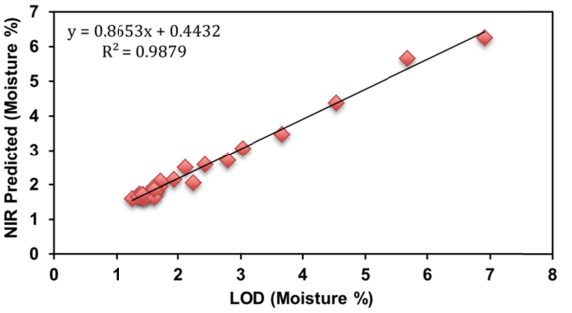

Figure 5. Regression plot between the moisture (%) predicted by NIR and the measured by LOD in the validation set using PLS model.

The specificity is the ability to identify the analyte (water) in the presence of other components which may be expected to be present. The specificity was demonstrated by the establishing the loading plot. The loading plot of the PC1 (the principal source of variation observed in the spectra, capturing 99.90% variability) shows maximum at the wavelength (1935 nm) which is corresponding to the characteristic OH combination band for water, as shown in Figure 3b.

To establish the accuracy of the proposed method, a paired *t*-test for independent samples was performed between the moisture content (%) predicted by the NIR method and those determined by the reference method (LOD). The analysis was carried out for the twenty-five validation samples. The test confirmed the absence of significant differences between the two methods; as the t_{exp} (1.23) for the NIR method was less than the t_{tab} (2.06) at the 95% confidence level.

The precision of the proposed method was determined by measuring the repeatability for the twenty-five validation samples. Repeatability was determined by repeating the analysis three times for each sample on the same day. The relative standard deviation (RSD%) was 2.50. The intermediate precision was not evaluated in this study as the moisture content of granules may increase with increasing the exposure time due to absorption of water from the surrounding atmosphere. Therefore, the developed NIR method for determination the moisture content of granules was successfully validated in accordance with ICH guidelines.

4. Conclusion

The first objective of this study was to apply the Plackett-Burman design for screening of process variables in FBG and study the influence of process variables on granules properties. The results obtained from the PB design revealed that the atomizing pressure and the airflow rate are the process variables that have strong influence on the granules properties. The results also indicated that the increase of airflow rate in the spraying phase with atomizing pressure allows us to obtain fine granules (small granule mean diameter) with more broadly granules dispersed (large span) and better compressibility and flowability properties (low Carr's index and Hausner ratio). On the other hand, the increase of airflow rate in the drying phase leads to granules with poor flowability. The moisture content of the granules is negatively affected by the atomization pressure, airflow rate in spraying phase and inlet air temperature in the drying phase. The second objective of this study was to develop and validate a NIR method to determine the moisture content of granule in the FBG. For this purpose, a partial least squares model for the NIR was applied. The proposed PLS model was fitted and their predictive performance was evaluated by traditional chemometric criteria. The root mean square error of prediction was 4.15% with 2 latent variables. The proposed PLS model for the NIR spectroscopy was successfully validated in accordance with ICH guidelines. The results obtained by the proposed NIR method were compared with those of the reference LOD method using a paired *t*-test. No significant difference has been observed. Therefore, the proposed NIR method was successfully applied for determination the moisture content of granules in FBG.

Acknowledgements

The authors would like to acknowledge the Faculty of Pharmacy, Misr International University for the financial support as well as the School of Pharmacy, University of Maryland. Special thanks to Dr. Stephen Hoag for his support, technical assistance and interest.

References

[1]. Appelgren, C. *Drug Dev. Ind. Pharm.* **1985**, *11(2-3)*, 725-741.
[2]. Burggraeve, A.; Monteyne, T.; Vervaet, C.; Remon, J. P.; De Beer, T. *Eur. J. Pharm. Biopharm.* **2013**, *83(1)*, 2-15.
[3]. Aulton, M. E. The science of dosage form design, Churchill Livingstone, Spain, 2002.
[4]. Bouffard, J.; Dumont, H.; Bertrand, F.; Legros, R. *Int. J. Pharm.* **2007**, *335(1)*, 54-62.
[5]. Tomuta, I.; Alecu, C.; Rus, L. L.; Leucuta, S. E. *Dev. Ind. Pharm.* **2009**, *35(9)*, 1072-1081.
[6]. Djuris, J.; Medarevic, D.; Krstic, M.; Vasiljevic, I.; Masic, I.; Ibric, S. *Sci. World J.* **2012**, *2012*, 1-10.
[7]. Martens, H.; Naes, T. Multivariate Calibration, John Wiley & Sons. Chichester, UK, 1989.
[8]. Tabasi, S. H.; Fahmy, R.; Bensley, D.; O'Brien, C.; Hoag, S. W. *J. Pharm. Sci.* **2008**, *97(9)*, 4052-4066.
[9]. Siesler, H. W.; Ozaki, Y.; Kawata, S.; Heise, H. M. Near-infrared spectroscopy: principles, instruments, applications, John Wiley & Sons, 2008.
[10]. Williams, P.; Norris, K. Near-infrared technology in the agricultural and food industries. 1987: American Association of Cereal Chemists

Inc., 1987.
[11]. Osborne, B. G.; Fearn, T.; Hindle, P. H. Practical NIR spectroscopy with applications in food and beverage analysis, Longman Scientific and Technical, 1993.
[12]. Frake, P.; Greenhalgh, D.; Grierson, S. M.; Hempenstall, J. M.; Rudd, D. R. *Int. J. Pharm*. **1997**, *151(1)*, 75-80.
[13]. Rantanen, J.; Lehtola, S.; Rämet, P.; Mannermaa, J. P.; Yliruusi, J. *Powder Technol. 1998*, *99(2)*, 163-170.
[14]. Findlay, P. W.; Peck, G. R.; Morris, K. R. *J. Pharm. Sci.* **2005**, *94(3)*, 604-612.
[15]. Hartung, A.; Knoell, M.; Schmidt, U.; Langguth, P. *Drug Dev. Ind. Pharm.* **2011**, *37(3)*, 274-280.
[16]. Obregon, L.; Quinones, L.; Velazquez, C. *Control Eng. Pract.* **2013**, *21(4)*, 509-517.
[17]. Kona, R.; Qu, H.; Mattes, R.; Jancsik, B.; Fahmy, R. M.; Hoag, S. W. *Int. J. Pharm.* **2013**, *452(1)*, 63-72.
[18]. USP 30 - NF 25. United States Pharmacopeial Convention, Rockville, MD, 2007.
[19]. Shawky, A.; Ibrahim, A.; Salem, M. Y.; El Gindy, A. E. *Am. Chem. Sci. J.* **2014**, *4(1)*, 24-37.
[20]. Szostak, R.; Mazurek, S. *J. Mol. Struct.* **2004**, *704(1)*, 235-245.
[21]. Mazurek, S.; Szostak, R. *J. Pharmaceut. Biomed.* **2006**, *40(5)*, 1235-1242.
[22]. International Conference on Harmonisation (ICH) of technical Requirements for Registration of Pharmaceuticals for Human Use, Validation of Analytical Procedures, Geneva, 2005.
[23]. Peinado, A.; Hammond, J.; Scott, A. *J. Pharmaceut. Biomed.* **2011**, *54(1)*, 13-20.
[24]. De Bleye, C.; Chavez, P. F.; Mantanus, J.; Marini, R.; Hubert, P.; Rozet, E.; Ziemons, E. *J. Pharmaceut. Biomed.* **2012**, *69*, 125-132.
[25]. Hu, X.; Cunningham, J.; Winstead, D. *J. Pharm. Sci.* **2008**, *97(4)*, 1564-1577.
[26]. Otsuka, T.; Iwao, Y.; Miyagishima, A. *Int. J. Pharm.* **2011**, *409(1)*, 81-88.